# Modifying a Polystyrene/Poly(methyl methacrylate) Interface with Poly(styrene-*co*-methyl methacrylate) Random Copolymers

**Mohan Sikka,[†] Nicole N. Pellegrini,[†] Edward A. Schmitt,[‡] and Karen I. Winey*,[†]**

*Department of Materials Science and Engineering and Laboratory for Research on the Structure of Matter, University of Pennsylvania, Philadelphia, Pennsylvania 19104-6272, and The Rohm and Haas Company, Bristol, Pennsylvania 19007*

*Received September 3, 1996; Revised Manuscript Received November 26, 1996*[⊗]

ABSTRACT: Joints of polystyrene (PS) and poly(methyl methacrylate) (PMMA) modified with ∼50 nm of poly(styrene-*co*-methyl methacrylate) random copolymer [P(S-*ran*-MMA)] were investigated. Copolymers having styrene compositions of $f_S = 0.48$ and $f_S = 0.73$ were used. Transmission electron microscopy reveals that the copolymers phase separate to form a distinct layer at the joint such that there is an interface with each homopolymer. Interfacial fracture toughness measurements, using the asymmetric double cantilever beam geometry, show a strong effect of the PS to PMMA sheet thickness ratio; that is, the phase angle influences the measured interfacial toughness. Reflection infrared spectroscopy on fracture surfaces indicates that the crack propagates at or near the PS/copolymer interface for all thickness ratios and for both copolymers. In-plane crazing was not observed in front of the crack tip for these systems. Rather, strengthening appears to be exclusively a consequence of oblique crazes in the more compliant PS sheet which form at 45° or 135° relative to the crack direction. Joints modified with P($S_{0.73}$-*ran*-MMA) exhibit denser oblique crazes than those modified with P($S_{0.48}$-*ran*-MMA), resulting in a higher measured fracture toughness at all sheet thickness ratios or phase angles.

## Introduction

Reinforcing homopolymer mixtures with copolymers continues to be an area of keen commercial and fundamental interest. Efficient interfacial agents should be easy to synthesize, thermodynamically favored to inhabit the joint region between the homopolymers, and effective in strengthening the joint. Block copolymers are one class of materials that have been shown to affect phase size and mechanical properties in polymer blends.[1,2] Block copolymer films (∼10−100 nm) coated between homopolymer sheets demonstrably increase the fracture toughness of the joint.[3,4] However, diblock copolymers remain expensive to synthesize commercially. Also, the possibility of other low-energy states, such as micelles or segregation to free surfaces, complicates the ideal picture of individual block copolymer chains moving in adequate numbers to the desired interfaces in a commercial process.[5,6]

Another promising route to interfacial strengthening is to use random copolymers. Random copolymers are relatively inexpensive to synthesize using standard free radical polymerization methods and do not form micelles. In a recent study, Kramer and co-workers[7] used the asymmetric double cantilever beam ("crack-opening") method to show that the compositionally symmetric poly(styrene-*ran*-2-vinylpyridine) random copolymer (i.e., having styrene composition $f_S \approx 0.5$) is remarkably effective at reinforcing the joint between homopolystyrene and homopoly(2-vinylpyridine). The effectiveness of the random copolymers decreased as $f_S$ increased or decreased relative to 0.5, that is, as the copolymer composition became asymmetric.

Brown's study[3] of poly(styrene-*co*-methyl methacrylate) block copolymers at polystyrene (PS)/poly(methyl methacrylate) (PMMA) joints included a small section on a commercial, polydisperse poly(styrene-*co*-methyl methacrylate) random copolymer [P(S-*ran*-MMA)] with an average styrene composition of $f_S = 0.7$. Copolymer films of thickness 10−40 nm coated between PS and PMMA sheets were found to significantly strengthen the joint. These results were from the so-called "static blade test", which consists of wedging a blade between homopolymer sheets and measuring the crack in front of the blade after 24 h. It is also important to note that these increased interfacial fracture toughness results were measured for a joint having equal PS and PMMA sheet thicknesses and with the PS sheet adhered to an Al plate.

Until recently, theoretical work[8,9] on AB random and alternating copolymers at the A/B homopolymer joint surmised a "stitch-like" organization for a single copolymer chain at the joint. Analytical or molecular dynamic approaches were utilized in these studies, and the free energy was found to be lowered when sections along the copolymer chain which were rich in A units formed loops on the A side of the joint and vice versa. Kramer and co-workers[7] rationalized their results for the PS:PVP system in terms of these theoretical predictions. They conclude that, for low coverage by a long, compositionally symmetric copolymer, the observed fracture toughness would imply about 10 connections across the PS/PVP joint for a random copolymer of length $N \approx 8000$ monomers.

An interesting issue that emerges from work in the Kramer group is that the observed strengthening persists when the random copolymer layer becomes comparable to or larger than the radius of gyration of the copolymer chains.[10] Brown's results using P($S_{0.70}$-*ran*-MMA) random copolymers at PS/PMMA joints are similar; interfacial toughness continues to increase as the copolymer layer thickness becomes 2 and 4 times the average radius of gyration of the copolymer chains (∼10 nm). These results cannot adequately be explained by the "stitch" model, because random copolymers in "thick" layers cannot cross between the A and

* To whom correspondence should be addressed at the Department of Materials Science and Engineering.
[†] University of Pennsylvania.
[‡] The Rohm and Haas Co.
[⊗] Abstract published in *Advance ACS Abstracts,* January 15, 1997.

S0024-9297(96)01302-2 CCC: $14.00 

**Table 1. Characteristics of Random Copolymers and Homopolymers**

| material | $M_w$[a] | $M_w/M_n$[a] | $f_S$[b] | $E$[c] (MPa) | $\sigma_\delta$[d] (MPa) |
|---|---|---|---|---|---|
| P($S_{0.48}$-*ran*-MMA) | 300 000 | 2.2 | 0.48 ± 0.02 | | |
| P($S_{0.73}$-*ran*-MMA) | 270 000 | 2.2 | 0.73 ± 0.02 | | |
| PMMA | 93 000 | 1.7 | 0 | 3300 | 100 ± 10 |
| PS | 220 000 | 2.3 | 1.0 | 3000 | 55 ± 5 |

[a] All molecular weights were measured using size exclusion chromatography with four mixed columns, THF solvent, and PS standards, except those for PMMA, which are measured using PMMA standards. [b] Measured using proton NMR. [c] Young's modulus taken from ref 4 was measured at a strain rate of $10^{-6}$ $s^{-1}$. [d] Crazing stress of the material from ref 4 was measured at a craze widening velocity of ~60 nm/s.

B homopolymer sheets.

Our own study on P(S-*ran*-MMA) random copolymers at PS/PMMA joints parallels work being done by Brown and co-workers.[11,12] An important goal of our work was to determine the predominant strengthening mechanism for copolymer layers coated at homopolymer joints. We deduce that the relative interactions of the copolymer with each homopolymer phase plays a role in determining the locus of fracture, and hence the apparent strength of the joint. We also find that the ratio of homopolymer sheet thickness ratio, or phase angle, profoundly affects the nature of the crack propagation observed and the interfacial fracture toughness measured.

## Experimental Section

**Polymer Synthesis.** Random copolymers of styrene and methyl methacrylate monomer units [P(S-*ran*-MMA)] were synthesized via free radical copolymerization in benzene initiated by benzoyl peroxide.[13] The reaction was terminated at less than 5% conversion by precipitating the polymer into methanol. Low conversions were used because we wanted to prevent composition drift within and between chains. Composition drift is expected to be especially significant in P(S-*ran*-MMA) when asymmetric monomer feed ratios are used in the reaction mixture and reactions are carried out to high conversions. This result follows from the reactivity ratios found for the monomers in the literature.[14] Low conversions for this reaction have the added advantage of producing copolymers with moderate polydispersities and eliminating the need for fractionation. PMMA and PS homopolymers were purchased from Scientific Polymer Products, Inc., and Polysciences, Inc., respectively. The molecular weights, polydispersities, compositions, and properties of the polymers used are reported in Table 1. Molecular weights and polydispersities of copolymers were determined using size exclusion chromatography, and compositions were determined from $^1$H NMR. As previously reported,[13,15] random copolymers with ~50 mol % styrene units have an alternating tendency, with only 10% of the triads occurring as homotriads. All polymers are atactic.

**Sample Preparation.** Homopolymer sheets were molded in a Carver hot press by placing PMMA or PS pellets in steel molds (3 in. square) between smooth photographic plates. The molds were of various thicknesses, ranging from 1.2 to 2.3 mm. Copolymer films of thickness ~50 nm were spin coated from toluene solutions on a silicon wafer and a glass slide at the same spinning speed (~2000 rpm). An ellipsometer (Rudolph AutoEl-II) was used to measure the film thickness on the spin-coated wafer. The glass slide coated with copolymer was immersed slowly in deionized water so that the copolymer film floated off. This film was carefully picked up on a PS sheet and dried at 50 °C under vacuum, after which a PMMA sheet was welded to the copolymer-coated PS sheet in air at 165 °C for 2 h under slight pressure. Concurrent neutron reflectivity studies indicate that this procedure is insufficient to achieve thermodynamic equilibrium at the joint.[16] (This observation limits the comparison between these fracture toughness experiments and our earlier equilibrium blend miscibility results.[22]) Samples ~8 mm wide were cut from the welded sheets using a circular saw with a diamond wafering blade (Buehler).

**Transmission Electron Microscopy (TEM).** The organization of the copolymer layers at the interface was examined using cross-sectional TEM. A cube measuring ~1.25 × 1.25 × 1.25 $mm^3$ was cut from the welded sheets which include the PMMA/PS joint. The cube was pretrimmed with a glass knife and then microtomed (55−70 nm) with a 35° Diatome diamond knife using a Reichert Ultracut S microtome. Sections were vapor stained with 0.5% aqueous ruthenium tetraoxide solution (Polysciences). The $RuO_4$ selectively stains styrene monomeric units in the copolymer and homopolymers, so that immiscible layers with different monomeric styrene densities exhibit distinct gray levels in the microscope. Specimens were imaged using a Philips 400T transmission electron microscope operated at 120 kV.

**Fracture Toughness Measurements.** The interfacial fracture toughness ($G_c$) of the welded joint was measured using the asymmetric double cantilever beam geometry. Samples measuring 50−80 mm in length and 8 mm in width were cut from the welded sheets. A single-edge razor blade, of thickness 0.23−0.3 mm, was inserted at the PS/PMMA joint and advanced at a steady rate of 0.25 mm/min using a vertical Instron Model 1125. Crack growth in a typical sample was permitted to stabilize for 10 min before data were collected for 30 min using a video camera (magnification 6−9×). The crack length, which is measured from the blade to the crack tip, was used to calculate the fracture toughness ($G_c$) of the joint using a standard equation.[17] Readings of the crack length were generally recorded every minute.

The literature[18,19] explains clearly why interfacial fracture mechanics is different from fracture in the bulk. Crack propagation through a bulk, amorphous, material does not have a preferred locus or directionality. The materials on either side of an interface, however, are different, and the interface provides a preferred direction of crack propagation. The implication is that in interfacial analysis the shear or mode II crack-tip stress patterns have to be considered in addition to the tensile or mode I stress patterns. The ratio between the shear and tensile crack-tip stresses can be described approximately by a phase angle or "mixity":

$$\psi = \tan^{-1}(K_{II}/K_I)$$

where $K_I$ and $K_{II}$ are the classical tensile and shear stress intensity factors, respectively. Using numerical methods and reasonable physical approximations, Xiao et al.[18,20] have calculated values of the phase angle for various sheet thickness ratios of dissimilar materials welded together. Note that these numerical calculations have not included a discreet copolymer layer between the two sheets of material, as will be the case in this study. In general when materials having a lower elastic modulus, such as PS, are joined with higher modulus PMMA or PVP, thickness ratios ~1 correspond to slightly positive values of the phase angle. This positive angle gives rise to a stress state at the crack tip which tends to deflect the crack toward the PS sheet instead of propagating the crack along the interface. The more compliant PS also has a low crazing stress, so that craze formation occurs in PS. (Crazing is a form of plastic deformation in glassy materials.) Crazing can contribute significantly to the measured fracture toughness, leading to values that are not considered representative of "true" interfacial strength.[21]

In studies where block copolymers were used to reinforce polymer joints,[3,4] the prescription to avoid these effects was to make the sample configuration asymmetric; that is, the stiffer (PMMA or PVP) sheet was made slightly thinner than the more compliant PS sheet. This leads to a somewhat negative phase angle, thus deflecting the crack toward the stiffer PMMA or PVP. Since these materials do not craze easily, the crack is forced to remain at or close to the interface, as desired.

For block copolymer reinforcement in the PS:PVP system, Xiao et al.[18] have published a detailed study of the effect of phase angle on $G_c$ at different copolymer coverages at the interface. In this study, the phase angle was varied from −15° to +5°, by varying the sheet thickness ratio ($h_{PS}/h_{PMMA}$) from ∼1.9 to 0.9. For low copolymer coverage to saturation coverage of the interface, the salient results were the following.

(a) Positive phase angles corresponding to $h_{PS}/h_{PVP} < 1.1$ led to oblique craze formation in the PS sheet at *forward* angles of ∼45°, corresponding to a situation where the maximum principal tensile stress acts normal to a plane oriented at ∼45° to the crack propagation direction. These crazes were considered to contribute significantly to the measured $G_c$ at positive phase angles, so that these values of $G_c$ were not considered representative of the interfacial strength.

(b) Negative phase angles, on the other hand, led to oblique craze formation in the PS sheet at *backward* angles of ∼45°, corresponding to a situation where the maximum principal tensile stress acts normal to a plane oriented at ∼135° to the crack propagation direction. Backward oblique crazes were found to contribute much less significantly to the measured $G_c$, particularly at small negative phase angles. Values of $G_c$ at small negative phase angles, then, were considered representative of the interfacial strength.

(c) Mechanical arguments were made for the initiation of both kinds of oblique crazes somewhat ahead of the crack tip, not directly at it.

(d) For sufficiently reinforced joints, true interfacial strengthening occurred when a craze formed immediately in front of the crack in PS. This craze was different from the oblique crazes in that its craze tip was close to or on the interface. It was conjectured that the breakdown of fibrils in this "horizontal" or "in-plane" craze, instead of in oblique crazes, was responsible for the propagation of the crack, although the thickening of the oblique craze was expected to contribute to the growth of the horizontal craze.

**Fourier Transform Infrared (FTIR) Microspectroscopy.** Infrared spectra were recorded using a Mattson Instruments Galaxy 6020 FTIR spectrometer equipped with a SpectraTech analytical infrared microscope and a liquid nitrogen cooled mercury cadmium telluride detector. For each sample, the crystal (single bounce, 45°, ZnSe) of a SpectraTech attenuate total reflectance (ATR) objective was brought into contact with the area to be sampled. The contact area was ∼200 $\mu$m in diameter. A spectral resolution of 4.0 cm$^{-1}$ was used, and 256 scans were summed to form each spectrum. Using the slit sampling method, the infrared radiation present at the ZnSe/polymer interface penetrates the polymer surface and is reflected back into the spectrometer. The radiant energy within the polymer decreases exponentially as a function of penetration depth. The point at which this energy reaches 1/e of the incident infrared radiation is referred to as the depth of penetration. The actual depth of penetration is wavelength dependent, but nominally 1−2 $\mu$m.

For comparison with fracture surfaces, FTIR spectra were collected from bare PS and PMMA sheets, as well as sheets coated with ∼50 nm of copolymer. Figure 1a shows a portion of the spectrum of a bare PMMA sheet, with a characteristic peak at ∼750 cm$^{-1}$. Parts b and c of Figure 1 are those of a PMMA sheet coated with ∼50 nm of P($S_{0.48}$-*ran*-MMA) and P($S_{0.73}$-*ran*-MMA), respectively. In addition to the 750 cm$^{-1}$ peak, a peak at 700 cm$^{-1}$ corresponding to the aromatic C−H out-of-plane deformation can be seen, indicating the presence of styrene monomer units (S) from the copolymer film at the surface.

Similarly, Figure 2a shows a portion of the spectrum of a bare PS sheet, with a peak characteristic of the styrene monomer unit at a wavenumber of ∼1600 cm$^{-1}$. Parts b and c of Figure 2 are those of a PS sheet coated with ∼50 nm of P($S_{0.48}$-*ran*-MMA) and P($S_{0.73}$-*ran*-MMA), respectively. An additional peak at 1730 cm$^{-1}$ corresponding to the carbonyl stretch appears, indicating the presence of methyl methacrylate monomer units (MMA) from the copolymer film coated at the surface. The intensity of the 1730 cm$^{-1}$ peak relative to the 1600 cm$^{-1}$ peak decreases as the styrene content of the copolymer increases.

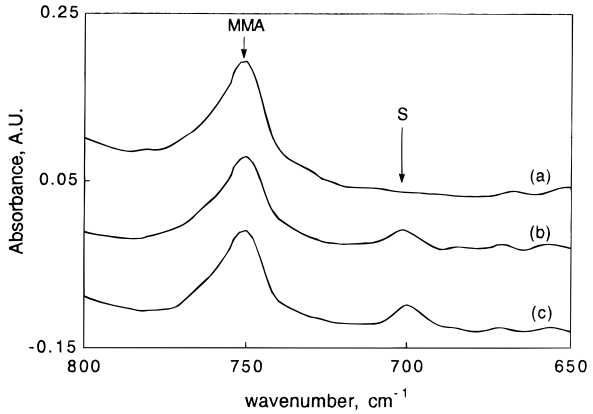


**Figure 1.** Reference FTIR spectra of PMMA sheets for comparison with fractured PMMA surfaces: (a) bare PMMA sheet, (b) PMMA sheet coated with ∼50 nm P($S_{0.48}$-*ran*-MMA) (a peak at 700 cm$^{-1}$ is visible, indicating styrene (S) monomer units in the copolymer), (c) PMMA sheet coated with ∼50 nm of P($S_{0.73}$-*ran*-MMA).

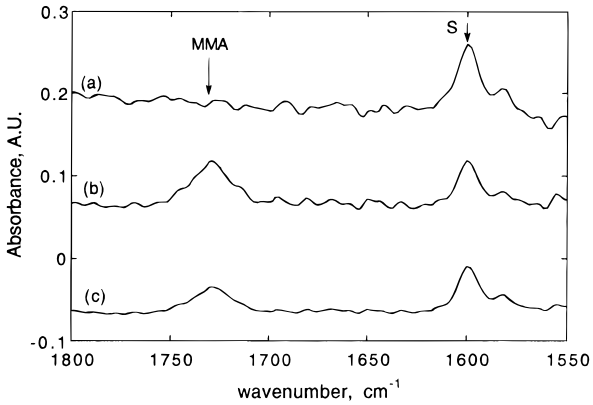


**Figure 2.** Reference FTIR spectra of PS sheets for comparison with fractured PS surfaces: (a) bare PS sheet, (b) PS sheet coated with ∼50 nm of P($S_{0.48}$-*ran*-MMA) (a peak at 1730 cm$^{-1}$ is visible, indicating methyl methacrylate (MMA) monomer units in the copolymer), (c) PS sheet coated with ∼50 nm of P($S_{0.73}$-*ran*-MMA) (the relative intensity of the 1730 cm$^{-1}$ peak decreases in intensity due to the lower MMA content of the copolymer).

## Results and Discussion

**Joints Modified with P($S_{0.48}$-*ran*-MMA).** Figure 3a shows TEM results for a bare PS/PMMA joint, with the two homopolymer phases clearly delineated by mass/thickness contrast. Figure 3b shows a TEM micrograph of a joint modified with a thick (∼1000 nm) layer of P($S_{0.48}$-*ran*-MMA), and Figure 3c shows a PS/PMMA joint with a thinner layer (∼50 nm) of P($S_{0.48}$-*ran*-MMA). The contrast between the three materials is adequate to conclude that copolymer layers ≥50 nm thick form a distinct phase at the joint, having a distinct interface with each homopolymer phase. We compared the ellipsometric thickness of the copolymer layers before welding with the value we can measure in the micrographs, and they were identical within experimental error, indicating that a negligible amount of copolymer has diffused into either homopolymer phase.

Fracture experiments on samples with ∼50 nm of P($S_{0.48}$-*ran*-MMA) at the joint showed a strong effect of phase angle. Numerical calculations have not been performed for the PS/PMMA system; thus, our experimental results will be presented in terms of the sheet

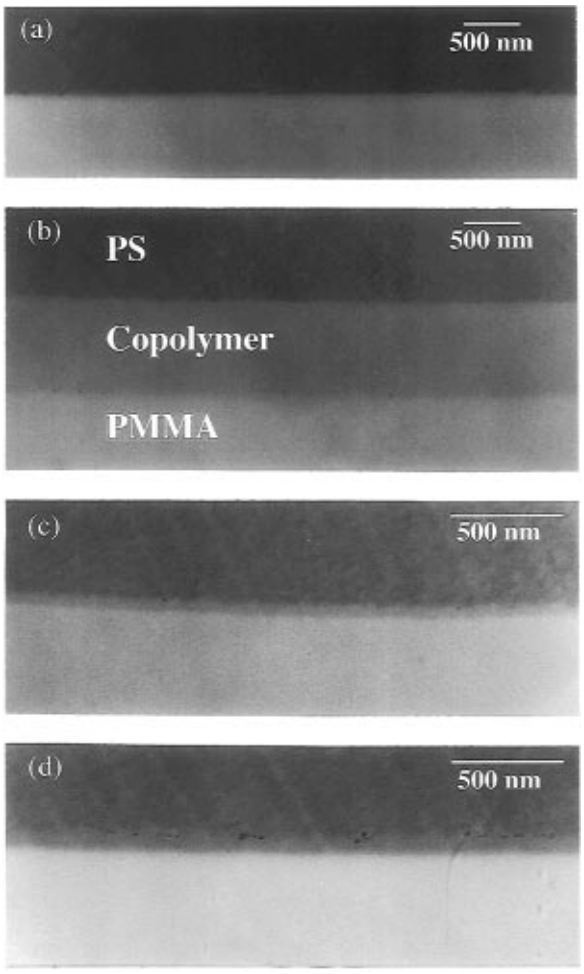


**Figure 3.** Transmission electron micrographs of PS/PMMA joints: joint without copolymer (a), joints modified with (b) ~1000 nm of P($S_{0.48}$-*ran*-MMA), (c) ~50 nm of P($S_{0.48}$-*ran*-MMA), and (d) ~50 nm of P($S_{0.73}$-*ran*-MMA).

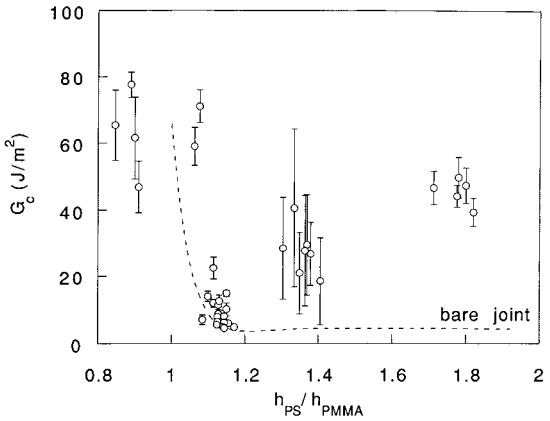


**Figure 4.** Fracture toughness results for PS/PMMA joints modified with ~50 nm of P($S_{0.48}$-*ran*-MMA) as a function of the PS to PMMA sheet thickness ratio, $h_{PS}/h_{PMMA}$. Also shown is the fracture toughness for unmodified (bare) PS/PMMA joints.

thickness ratio, $h_{PS}/h_{PMMA}$. (For comparison with the PS/PVP system, positive phase angles ($\psi > 0$) correspond to $h_{PS}/h_{PVP} < 1.1$, while negative phase angles ($\psi < 0$) correspond to $h_{PS}/h_{PVP} > 1.1$.) The measured interfacial fracture toughness, $G_c$, for several sheet thickness ratios ($h_{PS}/h_{PMMA}$) ranging from ~0.85 to ~2 is shown in Figure 4. The result for thickness ratios $\leq 1$ is as anticipated. As described in the Experimental Section, the phase angle is positive for these thickness ratios and the maximum principal tensile stress acts normal to a plane oriented ~ 45° to the crack propagation direction. This positive angle leads to the initiation of oblique crazes in PS, the material with the lower crazing stress, in the forward (i.e., crack propagation) direction. Such forward crazes can be seen under an optical microscope, such as those shown for joints with P($S_{0.73}$-*ran*-MMA) in Figure 12a. It should be pointed out that forward crazes are less distinct and not as closely spaced for joints modified with P($S_{0.48}$-*ran*-MMA), although craze fibril residue is clearly visible in Figure 6 for the sample with a thickness ratio of 0.89. The presence of these forward oblique crazes at thickness ratios $\leq 1$ leads to the high value of the fracture toughness measured.

When the thickness of the PS sheet is slightly larger than the PMMA sheet (ratio ~1.15), the fracture experiment shows a dramatically different result. A relatively long crack, without visible oblique crazes, is formed in front of the razor blade (see Figure 6). This thickness ratio appears to correspond closely to the situation where the in-plane stress state near the crack tip is purely hydrostatic; that is, the shear stress intensity factor $K_{II}$ (and hence the phase angle) $\approx 0$.[18] Oblique crazes in the PS are not formed under these conditions (ratio ~1.15), and a significantly lower value of $G_c$ results.

A third regime is found when the thickness ratio increases to ~1.35. Crack growth at the joint becomes unstable. Unlike the previous cases, the crack does not propagate at the same steady rate as the razor blade but, rather, begins to show "stick–jump" characteristics. For a time as the blade moves forward, the crack shortens and a band of crazes forms in front of or at the leading edge of the crack ("stick"). The crack then advances suddenly as the crack tip passes the band of crazes ("jump"). This behavior can be seen clearly in Figure 5, where we plot $G_c$ as a function of time for representative samples of different thickness ratios. For thickness ratios of 0.89 and 1.14 ($\psi < 0$ and $\psi \approx 0$, respectively), we see only random variation in $G_c$ with time. However, the sample with a thickness ratio of 1.36 shows an increasing value of $G_c$ in the stick portion of the cycle, followed by a drop to a lower value in the jump portion of the cycle. This stick–jump cycle repeats until the entire sample is cleaved. The relatively large variation in the $G_c$ value in 30 min of measurement leads to the large error bars for individual samples, as seen for thickness ratios ~1.35 in Figure 4.

Figure 6 shows sequential video frames of the fracture experiment at times corresponding to $t_1$ and $t_2$ as designated by arrows in Figure 5. For the samples with ratios of 0.89 and 1.14, little variation can be seen in the two frames. For the sample with a ratio of 1.36, frames taken 1 min apart show a large variation in the crack length between stick and jump behavior. The unstable crack propagation is also observed at the thickness ratio of ~1.8 with one significant variation; that is, the length that the crack advances in the jump portion decreases as the ratio becomes larger. This leads to oscillations in $G_c$ with time (Figure 5) that are somewhat less distinct for a sample with a thickness ratio of 1.71 as compared to the sample with a ratio of 1.36. This can be seen pictorially in Figure 6. The bands of crazes that are formed in samples with thickness ratios $\gtrsim 1.3$ can be clearly seen in the optical microscope when the fractured PS surface is viewed from the top (Figure 7). However, the side view of the

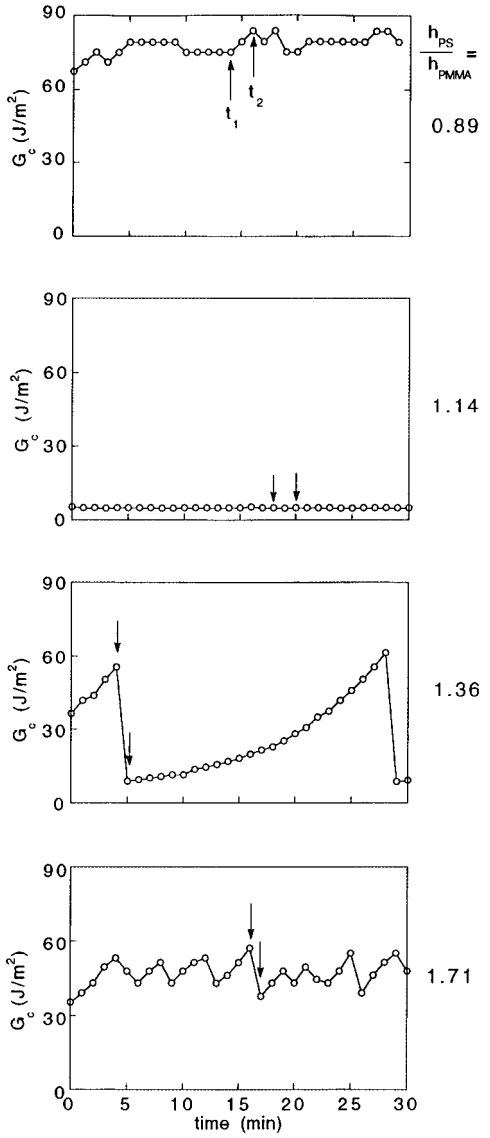


**Figure 5.** Time dependence of the fracture toughness for representative joints with ~50 nm of P($S_{0.48}$-*ran*-MMA) at various $h_{PS}/h_{PMMA}$ ratios. The arrows in each plot indicate sequential times ($t_1$, $t_2$) for which images of the fracture samples are displayed in Figure 6.

fractured PS surface does not reveal distinct oblique crazes in these bands that could be readily imaged in the optical microscope. We conjecture that the crazes are too short and/or too sparse to be readily observed.

FTIR-ATR spectroscopy of the surface was performed on both PS and PMMA sheets after fracture. Figures 8 and 9 show spectra from PMMA and PS samples, respectively, of varying thickness ratio. Also shown for comparison in each figure is the standard spectrum for ~50 nm of P($S_{0.48}$-*ran*-MMA) coated on a bare PMMA or PS surface which has not been welded or fractured, as was shown previously in Figures 1b and 2b. An immediate observation from these figures is that, after fracture, styrene can be detected on the fracture surfaces of PMMA sheets, whereas no significant MMA can be detected on the fracture surface of PS sheets. When crack propagation is accompanied by crazing in the PS (Figure 8b,d), the magnitude of the styrene signal from the PMMA sheet is larger than that from the copolymer layer alone (compare with Figure 8a). This result indicates that some of the PS sheet from near the PS/copolymer interface is on the PMMA sheet after fracture. On the other hand, when crack propagation occurs at the PS/copolymer interface without crazing (Figure 8c,e), the magnitude of the styrene signal from the PMMA sheet corresponds closely to that from the copolymer layer alone, implying fracture occurs at the PS/copolymer interface.

These results together clearly demonstrate that the locus of fracture lies at the PS/copolymer interface or within the PS sheet near the PS/copolymer interface. Our TEM, fracture, and FTIR results are schematically summarized in Figure 10, which has been drawn at an arbitrary size scale. The main point is to show that the copolymer/PMMA interface remains intact during fracture, and that the joint fails at or close to the PS/copolymer interface. The other salient observations are the following.

(a) A sheet thickness ratio ($h_{PS}/h_{PMMA}$) of 1.1−1.2 ($\psi \approx 0$) is required to avoid oblique crazes and to measure the intrinsic strength of the PS/P($S_{0.48}$-*ran*-MMA) interface as formed by modifying a PS/PMMA joint with 50 nm of P($S_{0.48}$-*ran*-MMA). As Figure 4 indicates the PS/P($S_{0.48}$-*ran*-MMA) interface is not significantly stronger than the bare PS/PMMA interface. This result indicates the absence of in-plane crazing ahead of the crack tip which would have strengthened the PS/copolymer interface relative to the PS/PMMA interface.

(b) For sheet thickness ratios >1.3 ($\psi < 0$) an irregular crack propagation, which we termed stick−jump, is observed. The stick region exhibits backward oblique crazes and PS craze debris on the PMMA sheet, while the jump region exhibits no oblique crazes and a fracture locus at the PS/P($S_{0.48}$-*ran*-MMA) interface. A similar irregular crack propagation has been previously reported, but only in the regime of positive phase angles, forward oblique crazes, and low block copolymer coverage.[18] Furthermore, unlike the interfaces modified with block copolymer which typically exhibit $G_c$ independent of phase angle at negative phase angle,[18] the interfaces modified with random copolymer show an increasing average $G_c$ as the sheet thickness ratio increases, that is, as the phase angle decreases.

(c) The average $G_c$ increases from its minimum value for $h_{PS}/h_{PMMA} < 1.1$ ($\psi > 0$) due to the creation of oblique forward crazes which subsequently leave PS debris on the PMMA sheet. This increase in effective $G_c$ is consistent with results for interfaces reinforced with a block copolymer as the phase angle increases.

**Joints Modified with P($S_{0.73}$-*ran*-MMA).** An electron micrograph of a PS/PMMA joint modified with ~50 nm of a P($S_{0.73}$-*ran*-MMA) with $f_s = 0.73$ is shown in Figure 3d. As with the P($S_{0.48}$-*ran*-MMA), a distinct copolymer phase is seen at the joint, with separate interfaces with each homopolymer phase. A comparison with ellipsometric thickness values shows once again that the majority of the copolymer remains at the joint.

Fracture results for these joints are shown in Figure 11 for varying PS to PMMA sheet thickness ratios. For comparison, the $G_c$ variation with thickness ratio for bare joints and for joints modified with P($S_{0.48}$-*ran*-MMA) is schematically included in this figure. Despite the noise in the data, some trends are noteworthy.

(a) In general, fracture toughness values are higher for joints modified with P($S_{0.73}$-*ran*-MMA) than for those with P($S_{0.48}$-*ran*-MMA) for the entire thickness ratio range studied.

(b) Large error bars, particularly around a thickness ratio of ~1.1, are caused by random variation in the measured crack length with time, not a systematic variation or stick−jump behavior discussed above for

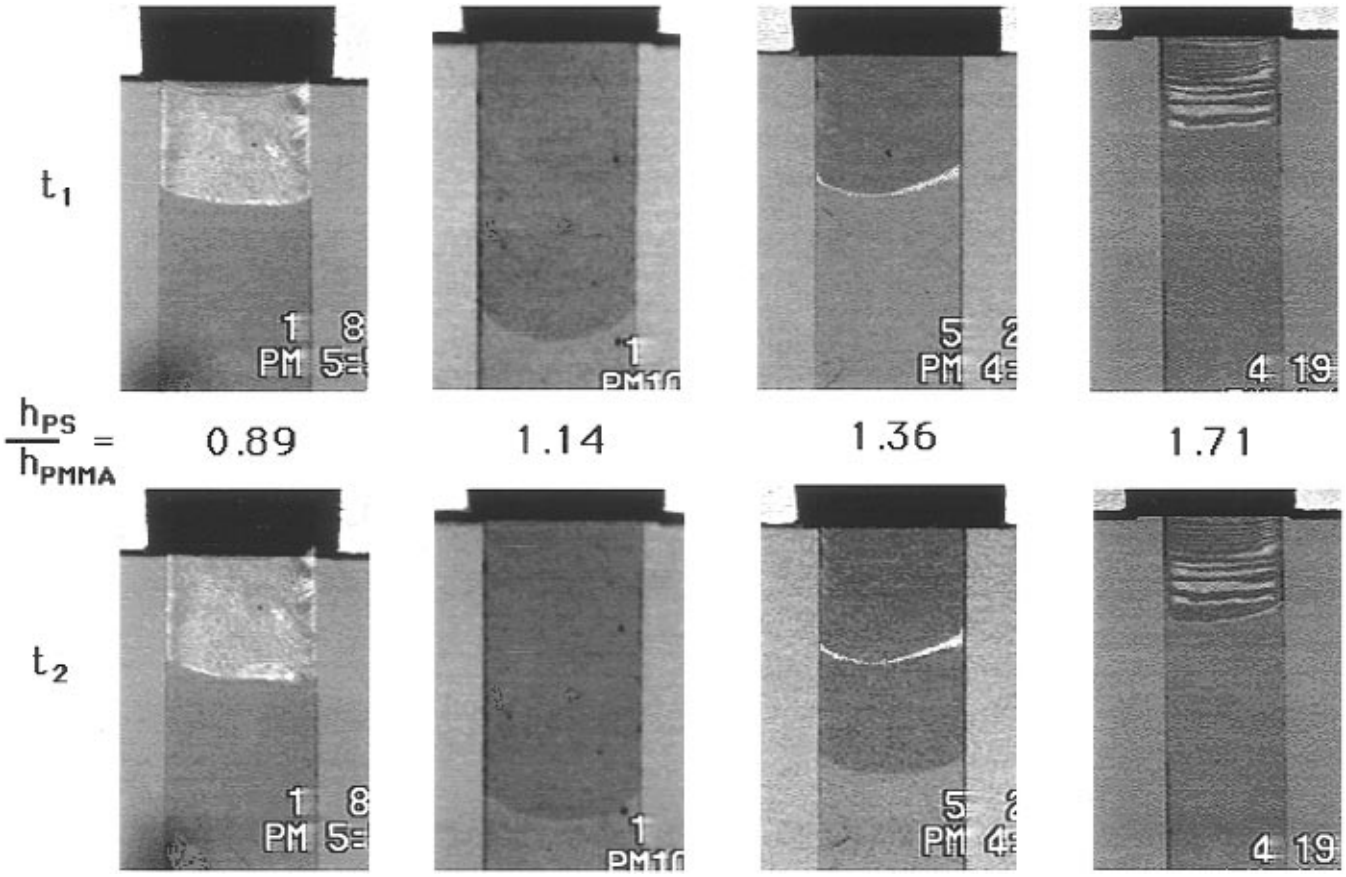


**Figure 6.** Video frames representative of the fracture experiments at indicated $h_{PS}/h_{PMMA}$ values. The upper and lower images correspond to times $t_1$ and $t_2$, respectively, as indicated in Figure 5. Fracture specimens are ~8 mm wide.

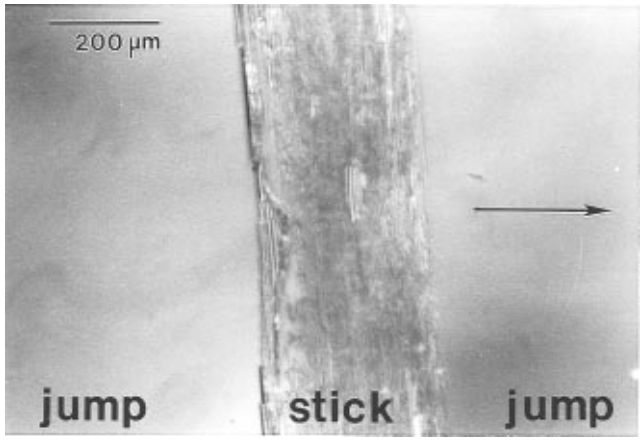


**Figure 7.** Optical micrograph of the top view of the PS surface after fracture. The joint was modified with ~50 nm of P($S_{0.48}$-*ran*-MMA), and $h_{PS}/h_{PMMA} = 1.3$. A band of crazes in the stick portion of the crack propagation can be readily seen. Jump portions look relatively smooth. The arrow identifies the direction of crack propagation.

thickness ratios of 1.36 and 1.71, Figure 5. Furthermore, stick−jump behavior was not observed at large $h_{PS}/h_{PMMA}$ values, and crack propagation was steady.

For P($S_{0.73}$-*ran*-MMA) layers, oblique crazes emanating from the fracture surface into the PS were readily visible from the side using optical microscopy (Figure 12). The directionality and density of the oblique crazes were found to depend on the sheet thickness ratio ($h_{PS}/h_{PMMA}$). For samples with a thickness ratio of $\lesssim 1.0$, corresponding to a positive phase angle, we observed forward pointing oblique crazes, similar to the case of the joint modified with P($S_{0.48}$-*ran*-MMA). It is noteworthy, however, that the forward pointing oblique crazes were more dense for joints with P($S_{0.73}$-*ran*-MMA), leading to higher measured values of $G_c$ as compared to joints with P($S_{0.48}$-*ran*-MMA). For example, at $h_{PS}/h_{PMMA} \approx 0.85$, $G_c$ is ~65 and ~130 J/m$^2$ for P($S_{0.48}$-*ran*-MMA) and P($S_{0.73}$-*ran*-MMA), respectively.

For thickness ratios $\gtrsim 1.3$, we observe backward pointing oblique crazes in the PS, similar to those seen for block copolymer reinforcement at negative phase angles.[18] At these thickness ratios, the directionality of the stress state in front of the crack tip is such that the maximum principal tensile stress acts normal to a plane oriented at ~135° to the crack propagation direction. This leads to the initiation of crazes in the PS in the backward direction. The crazes are sufficiently large and numerous to be clearly visible in the optical microscope (Figure 12b). Note that such backward pointing crazes were not readily seen for joints modified with P($S_{0.48}$-*ran*-MMA).

For thickness ratios between ~1.1 and 1.2, the noise in the fracture toughness data corresponds to a crossover from forward to backward oblique crazes, corresponding to a transition from $\psi > 0$ to $\psi < 0$. Recall that the true fracture strength of the joint in the absence of oblique crazes should be sampled at $\psi = 0$. However, as precisely as we were able to control the thickness ratio, all the samples showed oblique crazes. In fact, some samples in this thickness ratio range showed both forward and backward crazes in different sections of the fractured surface, implying that typical errors of 5% or less in sheet thickness are sufficient to change the directionality of the oblique crazes. It appears, then, that samples modified with P($S_{0.73}$-*ran*-MMA) are more susceptible to crazing than samples modified with

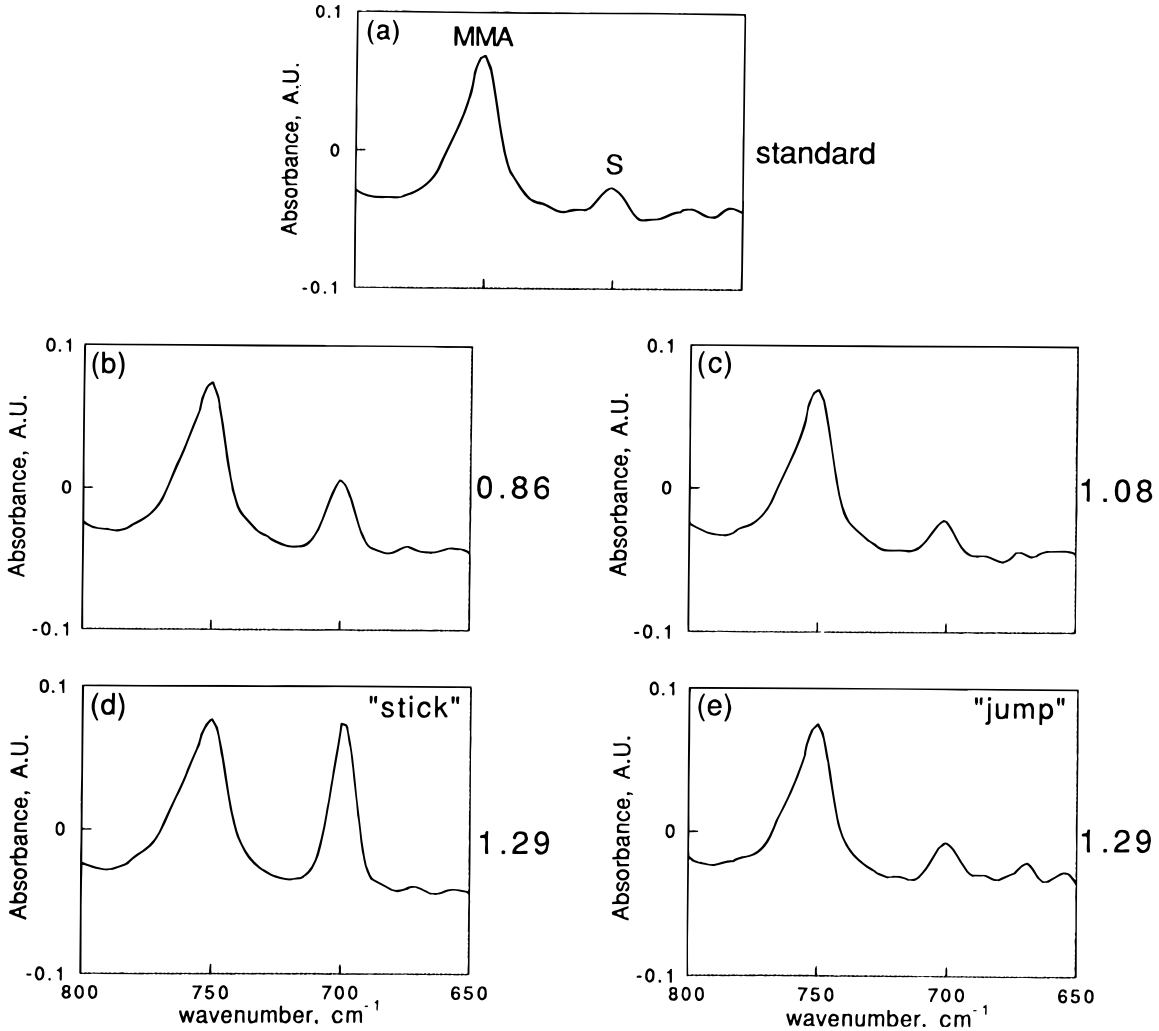


**Figure 8.** FTIR spectra from PMMA surfaces after fracture. All joints were modified with ~50 nm of P($S_{0.48}$-*ran*-MMA) and have $h_{PS}/h_{PMMA}$ values as indicated. For comparison the topmost plot marked "standard" is the result from a coated PMMA sheet which was not welded to a PS sheet.

P($S_{0.48}$-*ran*-MMA); we recall that, in the latter case, the "no oblique crazing" condition was readily achieved over this same thickness ratio. For P($S_{0.73}$-*ran*-MMA), the oblique crazes are smaller and less dense at $h_{PS}/h_{PMMA} \approx 1.1-1.2$ as compared with smaller or larger thickness ratios.

FTIR spectra from PMMA and PS fracture surfaces are shown in Figures 13 and 14. Also shown for comparison is the standard spectrum for ~50 nm of P($S_{0.73}$-*ran*-MMA) coated on a PMMA or PS sheet which has not been welded or fractured, as in Figures 1c and 2c. As with joints modified with P($S_{0.48}$-*ran*-MMA), S can be detected on the fracture surfaces of the PMMA sheets, whereas the amount of MMA detected on the fractured PS is small or negligible compared to the standard. When crack propagation is accompanied by significant oblique crazing in the PS (Figure 13b,d), the magnitude of the styrene signal from the PMMA sheet is larger than that from the copolymer layer alone (compare with Figure 13a). When the phase angle of the sample is ~0 and the size and density of crazes are small (Figure 13c), the magnitude of the styrene signal is correspondingly reduced.

A schematic representation of the fracture scenario in joints modified with 50 nm of P($S_{0.73}$-*ran*-MMA) is shown in Figure 15. The diagram is not to scale. As with P($S_{0.48}$-*ran*-MMA), the experimental evidence indicates that the joint continues to fail at or close to the PS/copolymer interface. The following are other key observations.

(a) Joints modified with P($S_{0.73}$-*ran*-MMA) exhibit a higher density of oblique crazes than joints modified with P($S_{0.48}$-*ran*-MMA). Thus, joints modified with P($S_{0.73}$-*ran*-MMA) exhibit higher fracture toughnesses over the entire thickness ratio (phase angle) range.

(b) The no oblique crazing condition, achieved relatively easily for samples modified with P($S_{0.48}$-*ran*-MMA) having thickness ratios of 1.1−1.2, was not be readily observed in samples with P($S_{0.73}$-*ran*-MMA). The oblique craze density did diminish somewhat between ratios of 1.1 and 1.2 for joints modified with P($S_{0.73}$-*ran*-MMA), but these few oblique crazes are apparently responsible for the increase in fracture toughness.

**Correlation with Homopolymer/Copolymer Miscibility and Interfacial Width.** Detailed miscibilty experiments[13,22] have been performed on blends of P($S_{0.48}$-*ran*-MMA) random copolymer and PS and/or PMMA homopolymer. These earlier studies indicate that P(S-*co*-MMA) random copolymers which are compositionally symmetric are partially miscible with PMMA and virtually immiscible with PS. This result is contrary to lattice arguments that predict comparable miscibilty with both homopolymers. Consequently, at high molecular weights a stable copolymer/PMMA interface will be broader than a PS/copolymer interface. This has been confirmed for P($S_{0.49}$-*ran*-MMA) copoly-

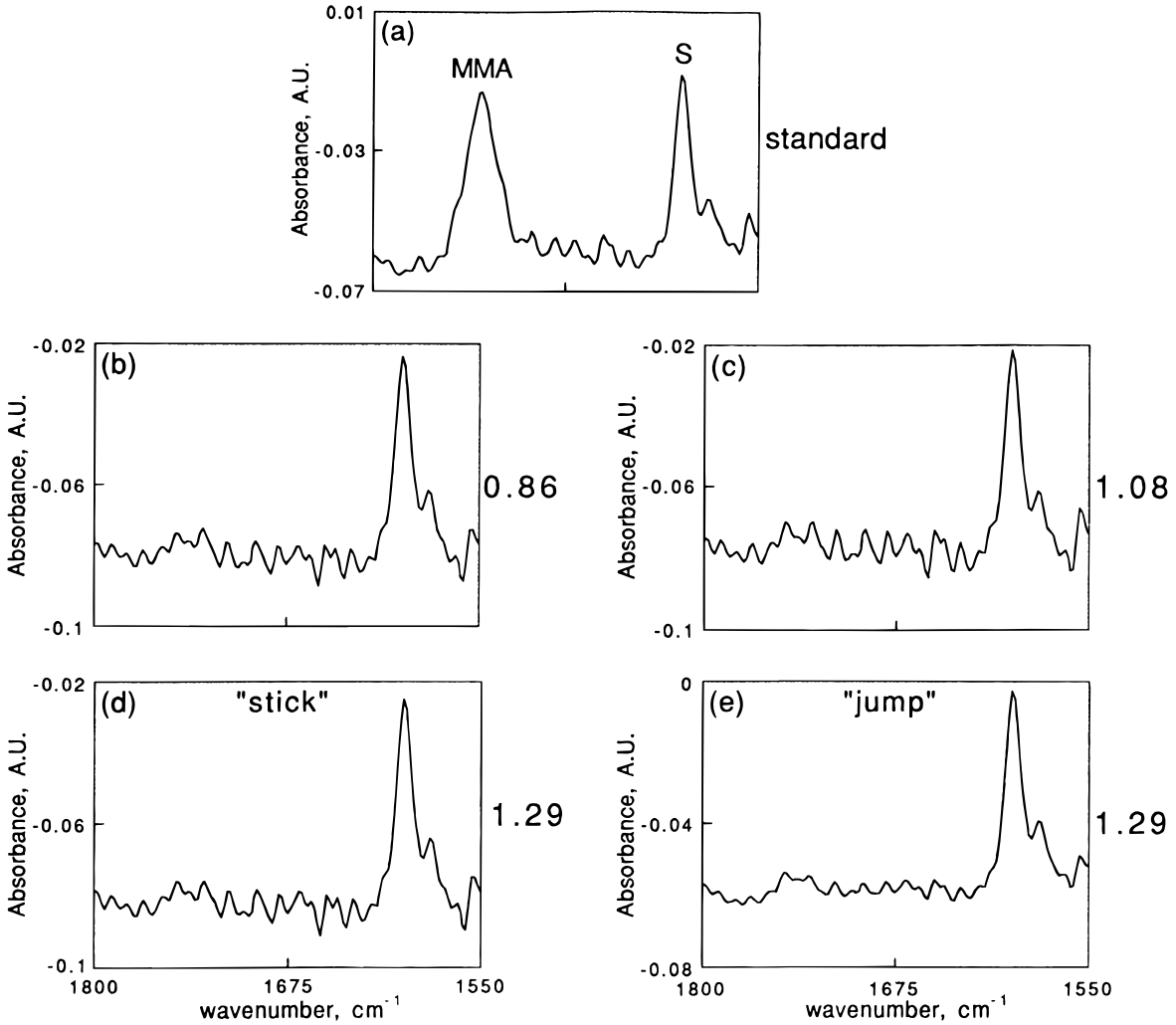


**Figure 9.** FTIR spectra from PS surfaces after fracture. All joints were modified with ~50 nm of P($S_{0.48}$-*ran*-MMA) and have $h_{PS}/h_{PMMA}$ values as indicated. For comparison the topmost plot marked "standard" is the result from a coated PS sheet.

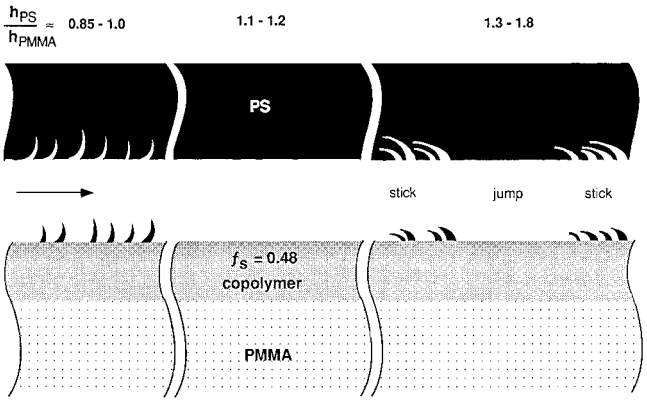


**Figure 10.** Schematic of crack propagation as a function of $h_{PS}/h_{PMMA}$ for joints modified with ~50 nm of P($S_{0.48}$-*ran*-MMA). The arrow identifies the direction of crack propagation.

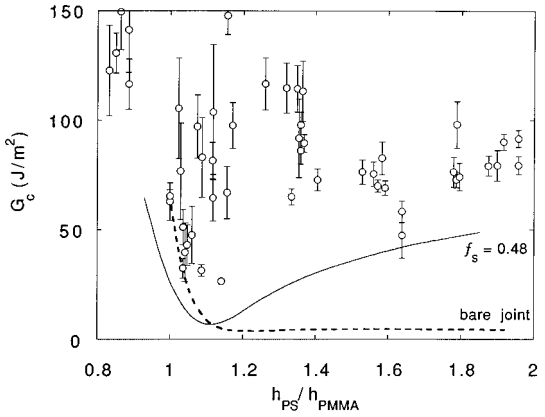


**Figure 11.** Fracture toughness results for PS/PMMA joints modified with ~50 nm of P($S_{0.73}$-*ran*-MMA) as a function of $h_{PS}/h_{PMMA}$. Also shown is the fracture toughness for unmodified (bare) PS/PMMA joints and PS/PMMA joints modified with ~50 nm of P($S_{0.48}$-*ran*-MMA).

mers using neutron reflection.[11,16] Our experimental results are consistent with these findings: the fracture trajectory lies at or close to the PS/copolymer interface for joints with a distinct layer of P($S_{0.48}$-*ran*-MMA), because this is the weaker of the two interfaces in the PS/P($S_{0.48}$-*ran*-MMA)/PMMA joint (See Figure 10).

Experimental evidence from further neutron reflectivity indicates that the PS/copolymer and the PMMA/copolymer interfaces become comparable in width at a copolymer composition greater than 50% styrene. It is not clear what role the copolymer/PMMA interface plays in the fracture mechanics of the joint. However, it seems logical that the broadening of the PS/copolymer interface for joints modified with P($S_{0.73}$-*ran*-MMA) leads to an increased ability to transfer stress from the joint to the compliant PS sheet. Larger stresses in the PS sheet for the joints modified with P($S_{0.73}$-*ran*-MMA) produce a higher density of oblique crazes in the PS. The crack trajectory appears to follow close to the PS/copolymer interface even at this styrene composition,

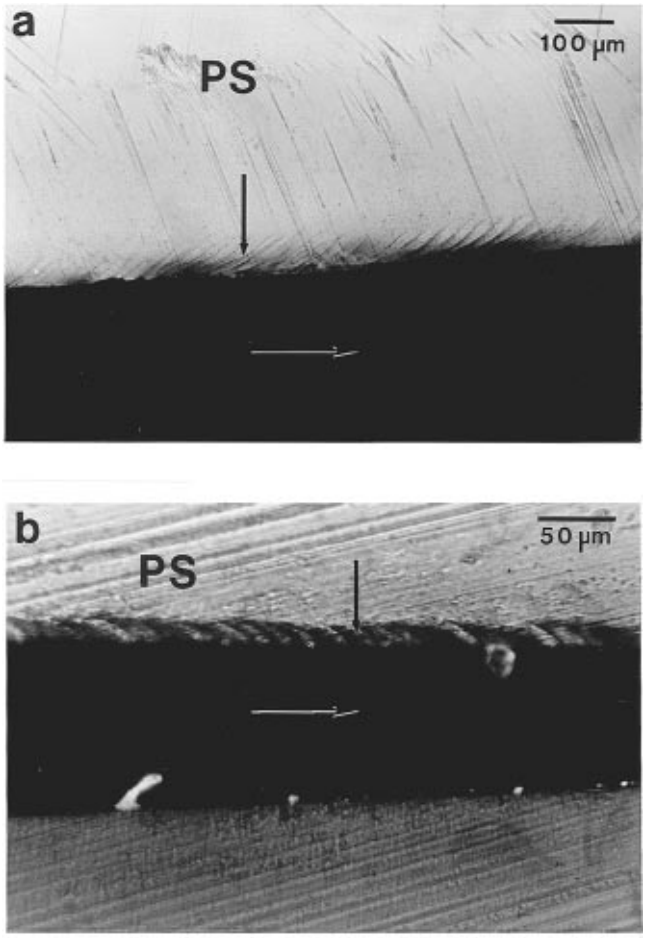


**Figure 12.** Side view optical micrographs of PS sheets after fracture for joints modified with ~50 nm of P($S_{0.73}$-*ran*-MMA): (a) $h_{PS}/h_{PMMA} = 0.85$; closely packed oblique crazes in the direction of crack propagation ("forward pointing") can be readily seen, (b) $h_{PS}/h_{PMMA} = 1.35$; closely packed oblique crazes opposite to the direction of crack propagation ("backward pointing") can be readily seen. Horizontal arrows indicate the direction of crack propagation. Vertical arrows point to the craze features.

although it seems intuitive that, at some higher styrene composition, the PMMA/copolymer interface will become the weakest link in the system and fracture will begin to take place there.

## Conclusions

Random copolymers P($S_{0.48}$-*ran*-MMA) and P($S_{0.73}$-*ran*-MMA) were used to modify the interface between PS and PMMA. TEM shows that copolymer layers 50 nm and thicker phase separate at the joint, with distinct interfaces with both PS and PMMA. This result is in agreement with a recent theoretical study[23] which indicates that the phase-separated state minimizes the free energy in these systems, so that a stitch-like organization of copolymer chains at the joint is energetically precluded at these coverages. For both copolymers FTIR experiments revealed that the locus of fracture within the joints was at the PS/copolymer interface or within the PS sheet near the PS/copolymer interface.

Fracture of these joints using the asymmetric double cantilever beam test showed a variety of distinct behaviors depending on the sheet thickness ratio, $h_{PS}/h_{PMMA}$, or phase angle, $\psi$, and the copolymer composition. At $h_{PS}/h_{PMMA} \leq 1.0$, corresponding to $\psi > 0$, forward pointing oblique crazes in the PS sheet emanate

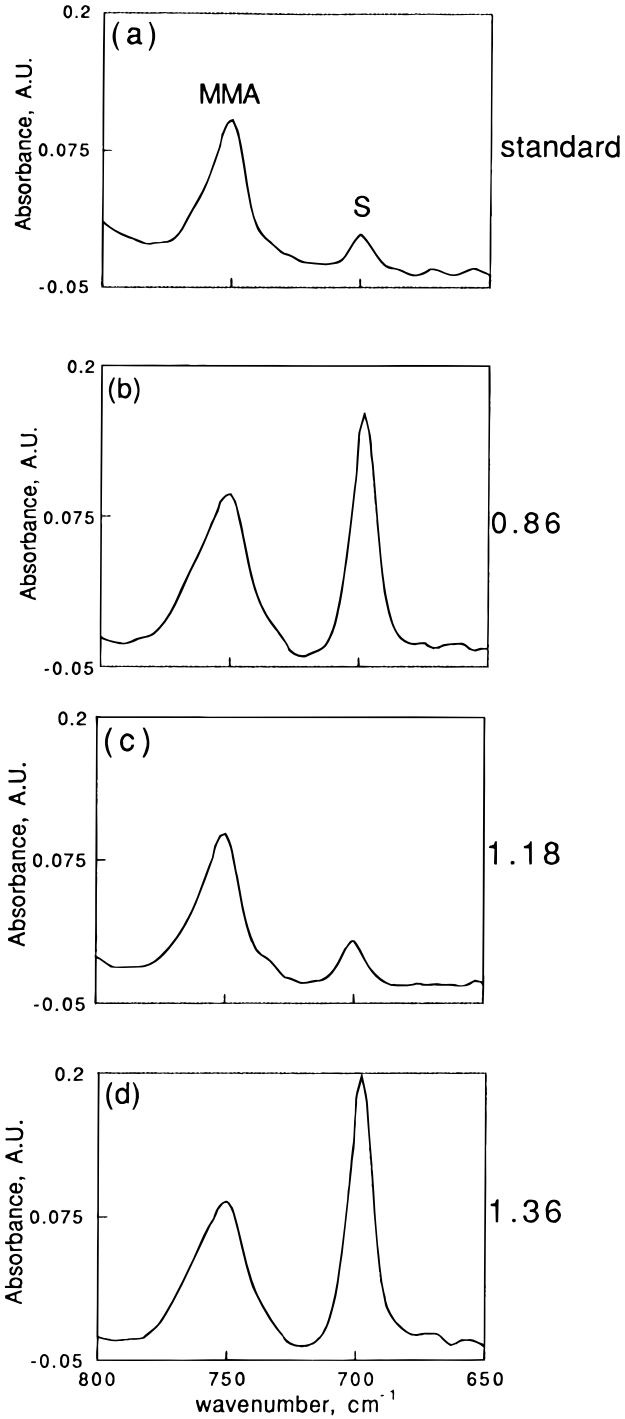


**Figure 13.** FTIR spectra from PMMA surfaces after fracture. All joints modified were with ~50 nm of P($S_{0.73}$-*ran*-MMA) and have $h_{PS}/h_{PMMA}$ values as indicated. For comparison the topmost plot marked "standard" is the result from a coated PMMA sheet.

from the fracture surface. These oblique crazes are more dense for joints modified with the styrene-rich random copolymer P($S_{0.73}$-*ran*-MMA). At $h_{PS}/h_{PMMA} \approx 1.15$, corresponding to $\psi \approx 0$, no oblique crazes are observed in joints modified with P($S_{0.48}$-*ran*-MMA), resulting in a low fracture toughness indicative of the PS/P($S_{0.48}$-*ran*-MMA) interface and comparable to the unmodified PS/PMMA interface. In this same range of thickness ratio, oblique crazes were observed in joints modified with P($S_{0.73}$-*ran*-MMA), giving a larger measured interfacial fracture toughness which is not solely indicative of the interfacial fracture toughness. Finally, at $h_{PS}/h_{PMMA} > 1.3$, corresponding to $\psi < 0$, backward

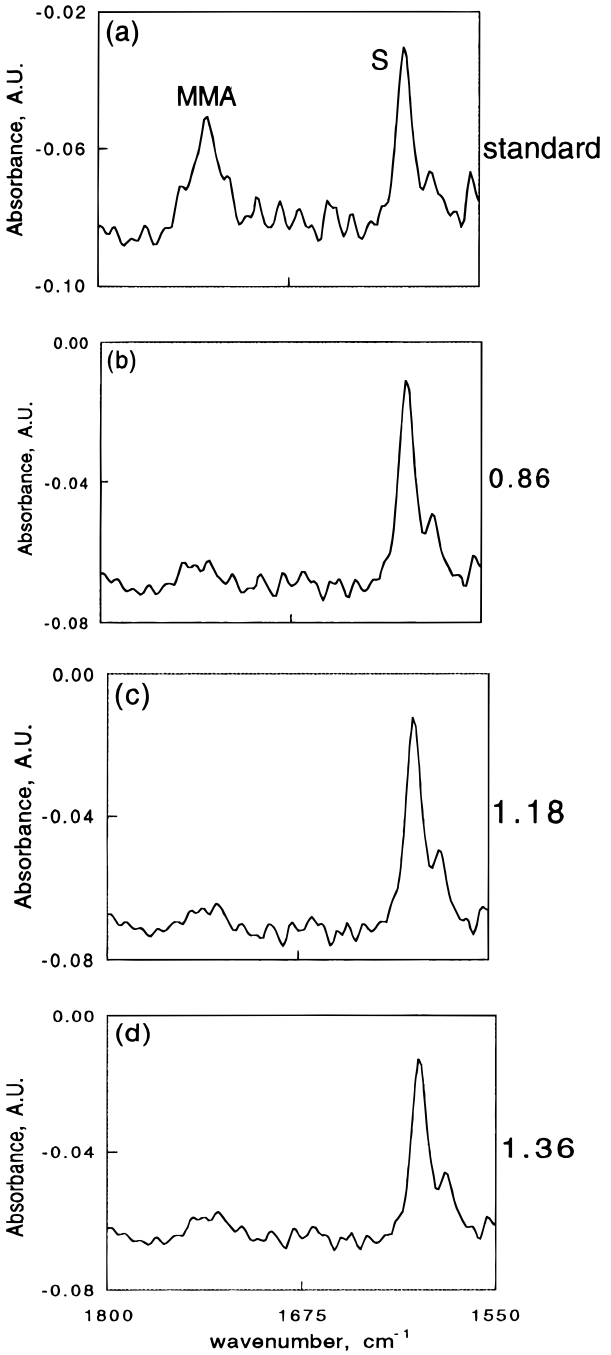


**Figure 14.** FTIR spectra from PS surfaces after fracture. All joints were modified with ~50 nm of P($S_{0.73}$-*ran*-MMA) and have $h_{PS}/h_{PMMA}$ values as indicated. For comparison the topmost plot marked "standard" is the result from a coated PS sheet.

crazes were observed either uniformly, as with joints modified with P($S_{0.73}$-*ran*-MMA), or intermittently, as with joints modified with P($S_{0.48}$-*ran*-MMA), showing stick−jump behavior. At all thickness ratios and for both copolymer compositions, strengthening of the joints appeared to be a result of the ability to transfer stress into the compliant PS to plastically deform the material into oblique crazes.

Overall, joints modified with ~50 nm of P($S_{0.73}$-*ran*-MMA) appeared tougher than joints with P($S_{0.48}$-*ran*-MMA), which reflects an increased ability of the higher styrene composition copolymer to transfer stress into the PS sheet. More stress transfer to the PS sheet is apparently responsible for the higher density of oblique crazes observed at all the sheet thickness ratios. Our

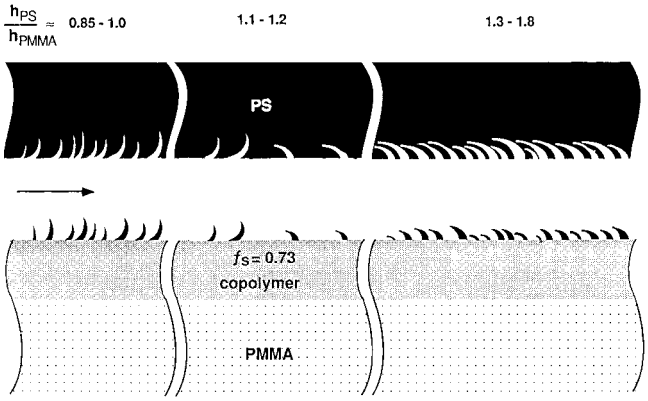


**Figure 15.** Schematic of crack propagation as a function of $h_{PS}/h_{PMMA}$ for joints modified with ~50 nm of P($S_{0.73}$-*ran*-MMA). The arrow identifies the direction of crack propagation.

recent neutron reflectivity results indicate that the PS/copolymer interface width increases as the styrene copolymer composition increases from 48 to 73 mol %, which concurs with our interpretation of the fracture toughness measurements.

Finally, our findings from the asymmetric double cantilever beam experiments illustrate the necessity of exploring a full range of sheet thickness ratios to establish the zero phase angle condition. For samples with distinct layers of random copolymers, the appropriate sheet thickness ratio is rather narrow. Our findings also show the value of recording the crack propagation as a function of time, so as to detect stick−jump or other intermittent behaviors. While the asymmetric double cantilever beam experiment has become a popular method used to study fracture mechanics of polymer interfaces, this study serves to demonstrate some of the possible pitfalls in the approach.

**Acknowledgment.** Professor Edward Kramer's generosity with equipment use, comments, and feedback are gratefully acknowledged. We would like to acknowledge useful discussions with Drs. Hugh Brown, Thomas Russell, and Anthony Dai. Thanks are also due to Mr. Alex Radin and Dr. Rollin Lakis of the LRSM and Dr. Sushil Satija of NIST. Mr. W. Loong Chen did some early fracture toughness experiments. Ms. Theresa E. Derderian initially designed the blade assembly for the crack opening test. Optical, ellipsometry, and spin coating experiments were done in Professor Russell Composto's laboratory at Penn. This work was supported by Grant NSF-DMR 93-07993, Grant NSF-DMR-YIA 94-57997, and a DuPont Young Professor Grant.

## References and Notes

(1) Fayt, R.; Jerome, R.; Teyssie, P. *J. Polym. Sci., Polym. Chem. Ed.* **1989**, *27*, 2823.
(2) Knaub, P.; Camberlin, Y.; Gerard, J. *Polymer* **1988**, *29*, 1365.
(3) Brown, H. R.; Char, K.; Deline, V. R.; Green, P. F. *Macromolecules* **1993**, *26*, 4155.
(4) Creton, C. R.; Kramer, E. J.; Hui, C.; Brown, H. R. *Macromolecules* **1992**, *25*, 1992.
(5) Dai, K. H.; Washiyama, J.; Kramer, E. J. *Macromolecules* **1994**, *27*, 4544.
(6) Shull, K. R.; Kramer, E. J.; Hadziioannou, G.; Tang, W. *Macromolecules* **1990**, *23*, 4780.
(7) Dai, C. A.; Dair, B. J.; Dai, K. H.; Ober, C. K.; Kramer, E. J.; Hui, C.; Jelinski, L. W. *Phys. Rev. Lett.* **1994**, *73*, 2472.
(8) Garel, T.; Huse, D. A.; Leibler, S.; Orland, H. *Europhys. Lett.* **1989**, *8*, 9.
(9) Yeung, C.; Balazs, A. C.; Jasnow, D. *Macromolecules* **1992**, *24*, 1357.
(10) Kramer, E. J. *Bull. Am. Phys. Soc.* **1996**, *41*, 213.

(11) Kulasekere, R.; Kaiser, H.; Ankner, J. F.; Smith, G. D.; Russell, T. P.; Brown, H. R.; Hawker, C. J.; Mayes, A. M. *Bull. Am. Phys. Soc.* **1996**, *41*, 318.
(12) Smith, G. D.; Russell, T. P.; Kulasekere, R.; Ankner, J. F.; Kaiser, H. *Macromolecules* **1996**, *29*, 4120.
(13) Galvin, M. E. *Macromolecules* **1991**, *24*, 6354.
(14) Greenley, R. E. In *Polymer Handbook*, 3rd ed.; Brandrup, J., Immergut, E. H., Eds.; John Wiley: New York, 1989; p II/153.
(15) Bovey, F. A. *J. Polym. Sci.* **1962**, ***62***, 197.
(16) Pellegrini, N. N.; Sikka, M.; Satija, S. K.; Winey, K. I. Manuscript in preparation.
(17) Kanninen, M. F. *Int. J. Fract.* **1973**, *9*, 83.
(18) Xiao, F.; Hui, C.; Washiyama, J.; Kramer, E. J. *Macromolecules* **1994**, *27*, 4382.
(19) Brown, H. R. *MRS Bull.* **1996**, *21*, 24.
(20) Xiao, F.; C -Y Hui; Kramer, E. J. *J. Mater. Sci.* **1993**, *28*, 5620.
(21) Brown, H. R. *J. Mater. Sci.* **1990**, *25*, 2791.
(22) Winey, K. I.; Berba, M. L.; Galvin, M. E. *Macromolecules* **1996**, *29*, 2868.
(23) Milner, S. T.; Fredrickson, G. H. *Macromolecules* **1995**, *28*, 7953.

MA961302H